NANOSCALE VISCOELASTIC CHARACTERIZATION USING TAPPING MODE AFM

L. Wang , K. Wu and S. I. Rokhlin
The Ohio State University
Nondestructive Evaluation Program
Edison Joining Technology Center
1248 Arthur E. Adams Drive, Columbus, OH 43221

INTRODUCTION

The tapping mode atomic force microscopy (AFM) has been widely used as a tool to image sample surfaces [1-3]. It has been modeled as a single degree-of-freedom nonlinear oscillator [4-11]. In this model, the tip-sample interactions are described by contact theory with adhesion (Johnson-Kendall-Roberts (JKR) theory) [12-14]. The viscoelasticity is considered as a friction force by adding a damping constant. Magonov and Elings [15] presented experimental results which show different phase sensitivity for stiff and soft samples. Anczykowski et al.[16] presented results on amplitude vs. tip-sample separation and showed the existence of hysteresis due to nonlinearity and the transition between attractive and repulsive forces. Kuhle et al [17] demonstrated experimentally the frequency response hysteresis and pointed out the effect of attractive force on this hysteresis using a linear interaction force approximation.

In this paper, we analyze the effects of damping and interaction forces (attractive and repulsive) on tapping mode AFM response. A simple analytical approximation is given to clarify this behavior. It shows that the phase and amplitude of cantilever vibration is dominated by the adhesion (attractive) or elastic (repulsive) force depending on sample properties and experimental conditions (amplitude ratio, driving frequency and driving amplitude). Instability or hysteresis may occur in the transition between these two states. The damping effect can significantly affect this transition. The analysis explains the hysteresis phenomena observed in the experimental frequency response and the effect of amplitude ratio in the AFM phase image [15].

EXPERIMENTAL OBSERVATIONS

A typical example of the experimentally measured vibration amplitude and phase frequency responses in tapping mode AFM is shown in Fig.1. The results were obtained using a commercial scanning probe microscope (NanoScope^{TM}) on a polyethylene sample. The frequency response is obtained by tuning the driving frequency slowly in the vicinity of the free resonance from high to low or from low to high as indicated by the arrows in the figure. The amplitude and phase of the free cantilever vibration are shown in the figure by

Review of Progress in Quantitative Nondestructive Evaluation, Vol. 18
Edited by Thompson and Chimenti, Kluwer Academic/Plenum Publishers, 1999

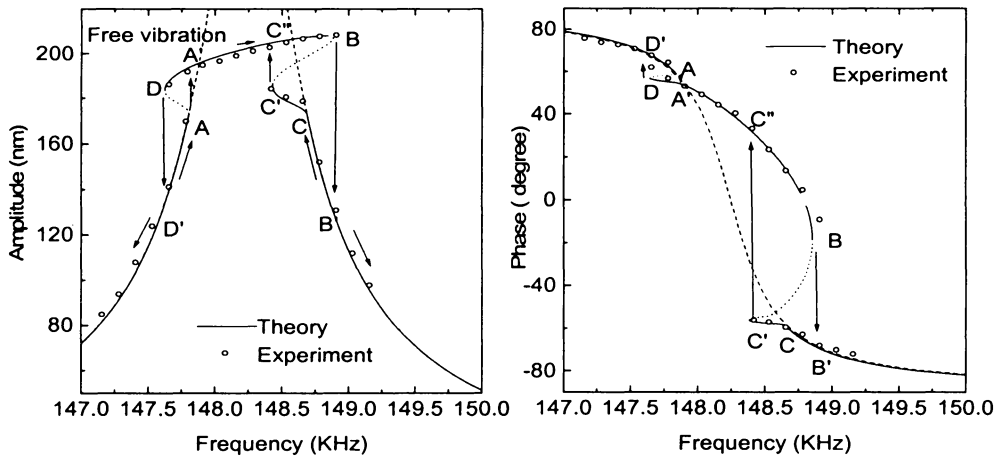

(a) amplitude (b) Phase

Figure 1. A typical frequency response in tapping mode AFM measured on polyethylene. The arrows show the frequency scanning directions.

dashed lines. As shown in Fig.1(a), from lower frequency to D' and from B' to high frequency there is free vibration; as the driving frequency increases to A, the amplitude suddenly increases to make the tip contact the surface. After the tip contacts the surface, amplitude increases as frequency increases. Then at frequency B which is higher than the resonance frequency the amplitude jumps to the free vibration value. The same phenomenon happens when the scanning frequency goes from high to low except the jump points are different. Similar phenomena have been observed by Anczykowski et al [16] and Kuhle et al. [17].

Figure 2 shows the experimental phase-amplitude ratio relations which are taken from Mogonov and Elings [15] for soft and stiff materials. As one can see, at high

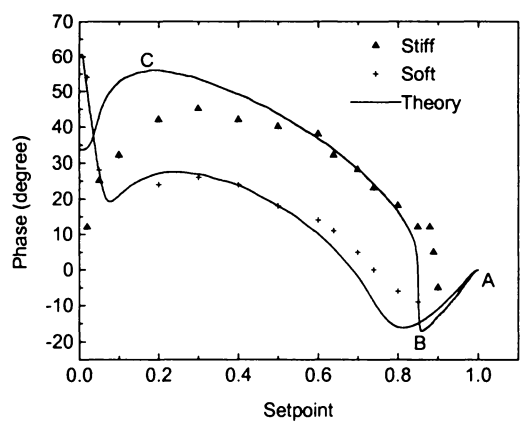

Figure 2. Phase versus setpoint amplitude ratio for soft and stiff materials. Experimental results are given by Magonov *et al.* [15].

amplitude ratio, when the tip touches the sample surface only slightly and the interaction is attractive, the phase is negative. As the amplitude ratio decreases, the effect of elastic force (repulsive) increases and the phase increases. The transition from negative to positive is very sharp for a stiff material. The phase for the stiff material is always higher than that for the soft material except near zero amplitude ratio where the phase for the soft material dramatically increases. Below we will investigate the effect of interaction forces on these behaviors.

THE SYSTEM MODEL AND APPROXIMATE SOLUTION

Model Description

A simple model of tapping mode AFM is a single degree-of-freedom nonlinear oscillator as shown in Fig.3. The vibrating system is described by the differential equation

$$\frac{d^2z}{d\tau^2} + 2\alpha\frac{dz}{d\tau} + (z + F(z)/k_c) = u_0\cos(\omega\tau). \qquad (1)$$

where $\omega_c = \sqrt{k_c/m}$, $\tau = t/\omega_c$ and α is the damping constant which includes free vibration damping α_0 and the losses occurring in the sample during the tip sample interaction. *F(z)* is the tip-sample interaction force.

The static tip-sample interaction forces have been described by the macroscopic continuum theories such as the Hertz, Johnson-Kendall-Roberts (JKR) and Derjaguin-Muller-Toporov (DMT) contact model. The relation between force and deformation in the DMT model is [10]:

$$F = K\sqrt{R}d^{3/2} - 2\pi wR,$$

where w is the surface energy, $K\sqrt{R}d^{3/2}$ is the repulsive Hertzian contact force and $1/K = 3((1-\nu_s^2)/E_s + (1-\nu_c^2)/E_c)/4$. ν_s, ν_c are the Poisson ratio of the sample and cantilever respectively

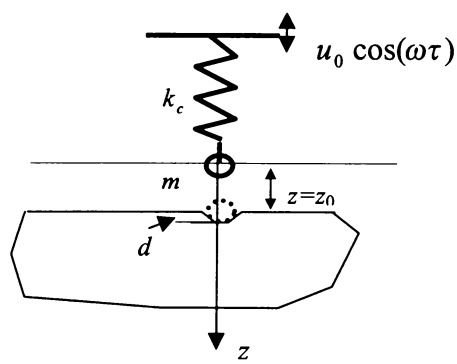

Figure 3. Model of tapping mode AFM.

and E_s, E_c are the Young's modulus of sample and cantilever respectively. R represents the tip radius. The deformation $d=z-z_0$. If one considers the attractive forces near the surface at $d<0$, the relation between force and deformation can be written as

$$F = \begin{cases} f(d) & d < 0 \\ K\sqrt{R}d^{3/2} - f_0 & d \geq 0 \end{cases}, \tag{2}$$

where $f(d)$ represents the van der Waals or other long range attractive force and as was given in [10]:

$$f(d) = \frac{-f_0}{\left(d/d_0 + 1\right)^2},$$

where f_0 is the adhesion force $2\pi wR$, $d<0$ and $d_0<0$ is a normalization constant.

When the tip impacts the material surface energy loss occurs due to viscoelasticity and adhesion, especially for polymers and biological materials. We account for these losses using the damping constant α_s. The radiation losses also can be accounted for by this constant. We add this damping constant in equation (1) $\alpha = \alpha_s + \alpha_0$ when deformation $d>d_0$.

Approximate Solution

The vibration amplitude may be considered nearly sinusoidal and the approximate solution can be written in the form :

$$z = A\cos(\omega\tau + \varphi).$$

Substituting this solution in eq.(1) and using the first order of the Krylov-Bogolubov-Mitropolsky asymptotic approximation [18], the amplitude A and phase φ can be found analytically as:

$$tg(\varphi) = \frac{\omega_e^2 - \omega^2}{2\alpha_e\omega}, \tag{3.a}$$

$$A(\omega_e, \alpha_e) = \frac{u_0}{\sqrt{(\omega_e^2 - \omega^2)^2 + 4\omega^2\alpha_e^2}}. \tag{3.b}$$

Damping α_e and resonance frequency ω_e are calculated as :

$$\alpha_e = \alpha_0 + \frac{2}{\pi}\int_0^{\theta_0} \alpha_s \sin^2(\theta) d\theta, \tag{4.a}$$

$$\omega_e^2 = 1 + \frac{2}{\pi A k_c}\int_0^{\theta_0} F(A\cos(\theta) - Z)\cos(\theta) d\theta, \tag{4.b}$$

where $\theta = \omega\tau + \varphi$ and $\theta_0 = \arccos(\frac{Z + d_0}{A})$.

RESULTS AND DISCUSSION

Amplitude and Phase Response to Driving Frequency

The experimental results shown in Fig.1(a,b) exhibit complicated hysteresis behavior appearing near resonance. The analytical solution described above has been used to analyze these phenomena. Fig.4(a,b) and Fig.5(a,b) show simulated frequency responses under different interaction conditions. Fig.4(a,b) clearly shows competition between attractive and repulsive forces controlling the nonlinear resonance behavior resulting from the cantilever surface interaction: 1) the adhesion force which leads to softening of the vibration system with amplitude increase and bending of the resonance curve to lower frequency (dashed curve in Fig.4(a,b)) and 2) the surface elastic repulsive force leading to stiffening of the vibration system with amplitude increase resulting in resonance curve bending to higher frequency, shown by the dotted curve in Fig4(a,b). The resulting solid line shows the combination of both behaviors (Fig. 4)

As one can see, there are two frequency ranges where three solutions (two stable and one unstable) exist. When the tip approaches the sample surface, the forces change as described by eq. (2). At $d<0$, the interaction force is attractive (adhesion force), and we assume in calculations that it affects the amplitude and phase of the cantilever vibration at $d \geq d_0$ and is zero at $d<d_0$. Two frequency ranges are dominated by the attractive force:

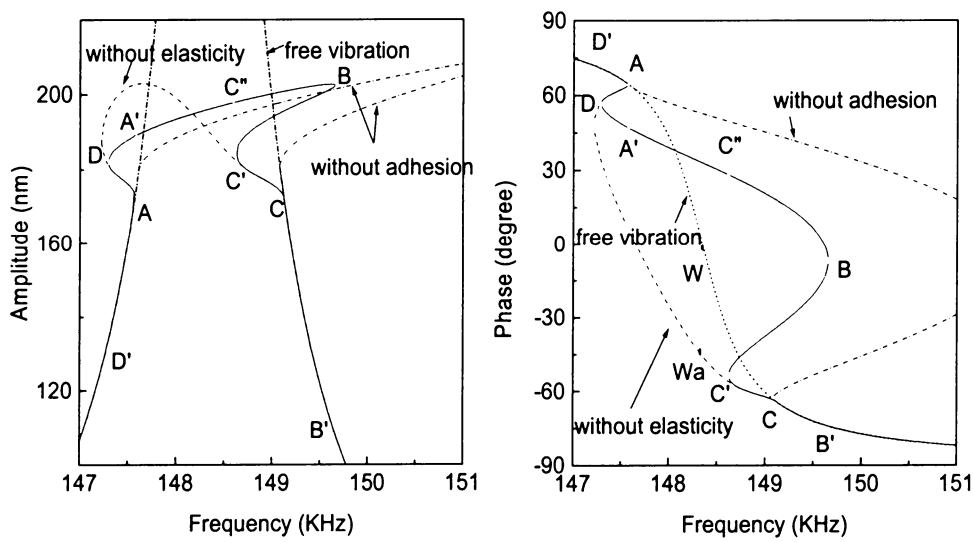

(a) amplitude (b) phase

Figure 4. Simulated frequency response in tapping mode.

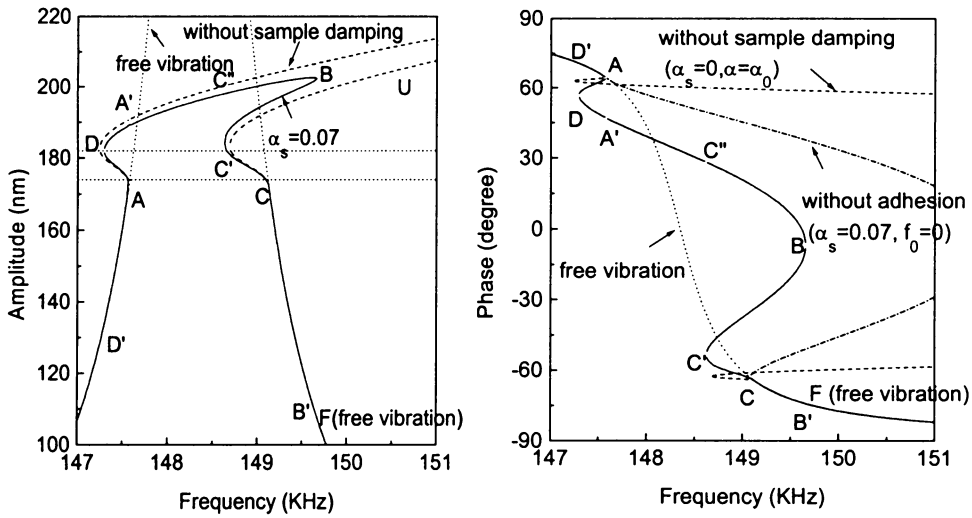

(a) amplitude (b) phase

Figure 5. Simulated frequency response in tapping mode.

DA and C'C with amplitude range shown between the two straight lines in Fig.4(a). When the frequency is swept from below toward the free resonance, the cantilever is drawn to the surface (the amplitude jumps from point A to point A') due to the attractive adhesion force. When the driving frequency is above the free resonance frequency, the vibration does not follow the free vibration part of the resonance curve (CB') even though the free vibration amplitude is smaller than the tip offset Z. Instead the amplitude first changes on the C"B segment of the curve and then jumps to point B' which is on the free vibration branch.

As the frequency is swept from above the free resonance, at position C the nonlinear resonance behavior is first dominated by the adhesion force and the amplitude increases slowly along CC'. At some distance the repulsive (elastic) force compensates the attractive force and the vibration amplitude increases suddenly (jumps) to point C" (since the free vibration amplitude is larger). At point C" it stabilizes on the resonance branch C"A' controlled by elastic forces. The amplitude changes to point D below resonance where it abruptly changes to the free vibration amplitude at point D'. Unlike the CC' segment, the solution segment AD corresponding to attractive force domination is unstable.

Comparison of the frequency responses with different damping shows that the transition BB' is significantly dependent on the damping and decreases rapidly to lower frequency and amplitude as the damping increases. At the same time the jump position DD' increases slightly as the damping increases while the transitions AA' and C'C" are only influenced slightly by the damping effect.

The sudden increase of the vibration amplitude A increases the effective interaction time θ_0 and, as follows from eq (4a), the effective damping α_e. However, the effective damping increase will decrease the vibration amplitude as follows from eq.3b. By smoothing the amplitude variation, the damping effect decreases the unstable vibration range and smooths the transition between the two states dominated by adhesion and elasticity forces. As shown in the phase response in Fig.5(b), without damping, the phase is almost constant with frequency and changes from positive to negative phase at very high

frequency which is out of the scale range in Fig. 5(b). This phase change at resonance is common for small damping and happened in this case due to the nonlinearity at $\omega = \omega_e$ instead of $\omega = \omega_0$. Similar to the transition BB' (fig.5b) it occurs by a jump on the stable free vibration branch (F) instead of the unstable branch (U) of the phase characteristic. Since $\alpha_0 << 1$, the effective damping α_e is dominated by sample damping α_s (eq. 4.a). The sample damping α_s increases the effective damping significantly and leads to the shape of the phase characteristic shown by the solid line in fig. 5(b). Therefore the phase variation is significantly affected by the damping effect.

Phase Response on Interaction Forces

Figure 6 shows simulated dependences of phase versus amplitude ratio for different values of interaction forces and damping. For zero sample damping $\alpha_s = 0$, the phase is positive for tip/sample interaction controlled by repulsive (elastic) forces (top curve F_+ is for zero attractive (adhesion) force f_0=0). The phase is negative for interaction controlled by attractive forces. The phase for zero elastic forces (K=0) is exactly equal in value and opposite in sign (F_- curve).

For very small material damping and nonzero elastic and adhesion interaction forces, the phase is on the lower F_- or upper F_+ phase curves independently of the actual value of these forces. With decrease of A/A_0 ratio, the transition occurs from the bottom F_- adhesion-dominated interaction curve to the top F_+ elastic-dominated interaction curve. The value of surface stiffness K at which the transition occurs is shown in the figure. One concludes that the phase characteristic is absolutely insensitive to the magnitude of the interaction forces, however it is very sensitive (phase inversion) to transition from attractive to repulsive force control oscillation as the tip approaches the surface during tapping. As shown in Fig.6, the phase is significantly dependent on the damping. As damping increases, the phase decreases and shifts from repulsive force control F_+ to attractive force control F_-. The damping makes the specimen surface become effectively "stiff" which leads to small deformation. At small deformation, the dominant interaction is the attractive force. Therefore the phase decreases and the negative regime increases as damping increases.

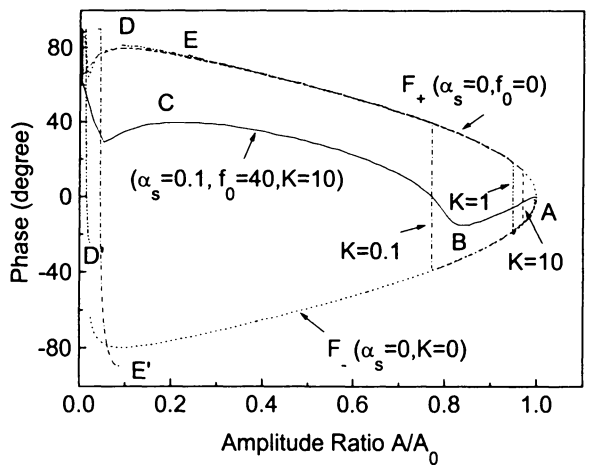

Figure 6. Phase versus setpoint amplitude ratio under different interaction terms.

CONCLUSION

By using an analytical model which includes the attractive, repulsive and damping forces, the complicated features in tapping mode AFM have been represented and supported by experiment. The AFM measured features are dominated by two regimes: adhesion force control or elastic force control. Due to the nonlinear character of the AFM vibration system, the transition between the two regimes depends on the system parameters and damping.

ACKNOWLEDGEMENTS

This work was sponsored by the Defense Advanced Projects Agency (DARPA) Multidisciplinary University Research Initiative (MURI), under Air Force Office of Scientific Research grant number F49620-96-1-0442.

REFERENCE

1. G. Binning , C. F. Quate and C. Gerber, Phys.Rev.Lett., 56, 930(1986).
2. M. Radmacher, R. W. Tillmann, M. Fritz and H. E. Gaub, Science, 257, 1900 (1992).
3. H. G. Hansma and J. H. Hoh , Annual Reviews of Biophysics and Biomolecular Structure, 1994.
4. D. Sarid, T. G. Ruskell, R. K. Workman and D. Chen, J. Vac. Sci. Technol. B 14(2), 864(1996).
5. C. A. Putman, K. O. V. der Werf, B. G. deGrooth, N. F. V. Hulst, and J. Greve , Applied Physics Letters, 64, 2454(1994).
6. J. P. Spatz, S. Sheiko, M. Moller, R. G. Winkler, P. Reineker and O. Marti, Nanotechnology, 40 (1995).
7. R. G. Winkler, J. P. Spatz, S. Sheiko, M. Moller, P. Reineker and O. Marti, Phys. Rev. B, 54, 8908(1996).
8. J. Chen, R. K. Workman, D.Sarid and R.Hoper, Nanotechnology, 5, 199 (1994).
9. J. Tamayo and R. Garcia, Langmuir, 12, 4430(1996).
10. N. A. Burham, O. P. Behrend, Foulevey, G. Gremand, P. J. Gallo, D. Gourdon, E. Dupas, A. J. Kulik, H. M. Pollock and G. A. D. Briggs, Nanotechnology , 8, 67(1997).
11. G.Y. Chen, R.J. Warmack, A. Huang, and T. Thundat, J. Appl. Phys., 78, 1465 (1995).
12. D. Maugis and B.Gauthier Manuel, J.Adhesion Sci.Technol., 8, 1311(1994).
13. K. J. Johnson, Contact Mechanics, Cambridge University Press,1985.
14. N.A.Burnham, R.J.Colton and H.M.Pollock, Nanotechnology, 4, 64-80 (1993).
15. S. N. Magonov, V. Elings and M. H. Whangbo, Surface Science, 375, 385-391(1997).
16. R. Anczykowski, D. Kruger and H. Fuchs, Phys. Rev.B, 53,15485(1996).
17. A. Kuhle, A. H. Sorensen and J. Bohr, J. Appl. Phys., 81,6562(1997).
18. N. Minorsky, Nonlinear Oscillations, D.Van Nostrand Company,1962.